16. THE DEADLY COMBINATION OF HEAT AND HUMIDITY IN INDIA AND PAKISTAN IN SUMMER 2015

Michael Wehner, Dáithí Stone, Hari Krishnan, Krishna AchutaRao, and Federico Castillo

We find that the deadly heat waves in India and Pakistan in 2015 were exacerbated by anthropogenic climate change. Although the impacts of both events were severe, the events themselves were not connected to each other.

Observations and Impacts. Andhra Pradesh, Telangana, and other southeastern Indian states suffered a deadly heat wave in late May and early June of 2015. Daily high temperatures exceeded 45°C in many places throughout India for several days in a row. In late June and early July, just a few weeks later, Pakistan also suffered from a deadly heat wave with similar daily high temperatures. Although the Pakistani heat wave occurred very soon after the Indian heat wave, they were distinct meteorological events. Ratnam et al. (2016) classify heat waves over India into two types, those that occur over north-central India and those that occur over coastal eastern India. The study finds that the former tend to be associated with anomalous blocking over the North Atlantic Ocean. Heat waves over coastal eastern India were found to be associated with westerly anomalies over the Indian landmass, thereby reducing the land–sea breeze along the coastal regions. Hence the Loo, a strong afternoon overland wind, brought hot and dry conditions to India (Fig. 16.1a). By late June, the Indian monsoon was well developed, curtailing these winds and terminating the heat wave (see www.tropmet.res.in/~lip/Publication/Scientific-Reports/RR-185.pdf). In Pakistan by this time, winds were onshore (Fig. 16.1b), and the unusually hot conditions were also unusually humid. The high numbers of deaths in both events are attributed not only to the weather conditions but also to institutional failures. Hospitals were overwhelmed with patients suffering from heat-related symptoms and at some point had to turn away patients (Salim et al. 2015). It is difficult to be precise about the ultimate number of fatalities associated with these heat waves, but upwards of 2500 excess deaths are estimated to have occurred in the Indian heat wave (Ratnam et al. 2016) and at least 700 alone in the Pakistani megacity of Karachi (Masood et al. 2015) with many more throughout the country.

To further characterize these heat waves, we have analyzed 1973–2015 subdaily (hourly and 3-hourly) temperature and heat index (Steadman 1979a,b) calculated from the HadISD v1.0.4.2015p quality controlled weather station dataset (Dunn et al. 2012). Heat index, one of several methods to measure the combined effect of temperature and humidity on human health, is a bicubic function of both variables intended to fit a model of a fully clothed adult (see Supplemental Material for its definition). Figures 16.1c,d show the daily maximum instantaneous heat index (thick red lines) and the temperature (thick black lines) associated with it during the heat waves in Hyderabad (in the Indian state of Telangana, WMO station number 431280) and Karachi (the largest city in Pakistan, WMO station number 417800). The pentadal averages of these daily maxima are shown with thin lines. Climatological averages over 1974–2014 are shown with horizontal dotted lines for May in Hyderabad and June in Karachi to show the events' relative severity. In Hyderabad, the daily maximum heat index was about 2°–4°C higher than temperature during the heat wave. In Karachi, this difference was about 7°–12°C, reflecting a much higher relative humidity. The first column of Table 16.1 shows representative values of temperature and heat index during the most severe periods of the 2015 heat waves drawn from Figs. 16.1c,d.

Figures 16.2a,b are scatterplots of relative humidity against temperature at the time of the daily maximum heat index value over the observational record of 1973–2015. Colored dots show the official U.S. NOAA advisory heat index levels of caution, extreme caution, danger, and extreme danger. In such hot climates, the 1974–2014 average daily maxi-

AFFILIATIONS: Wehner, Stone, and Krishnan—Lawrence Berkeley National Laboratory, Berkeley, California; AchutaRao—Indian Institute of Technology Delhi, Hauz Khas, New Delhi, India; Castillo—University of California at Berkeley, Berkeley, California

DOI:10.1175/BAMS-D-16-0145.1

A supplement to this article is available online (10.1175/BAMS-D-16-0145.2)

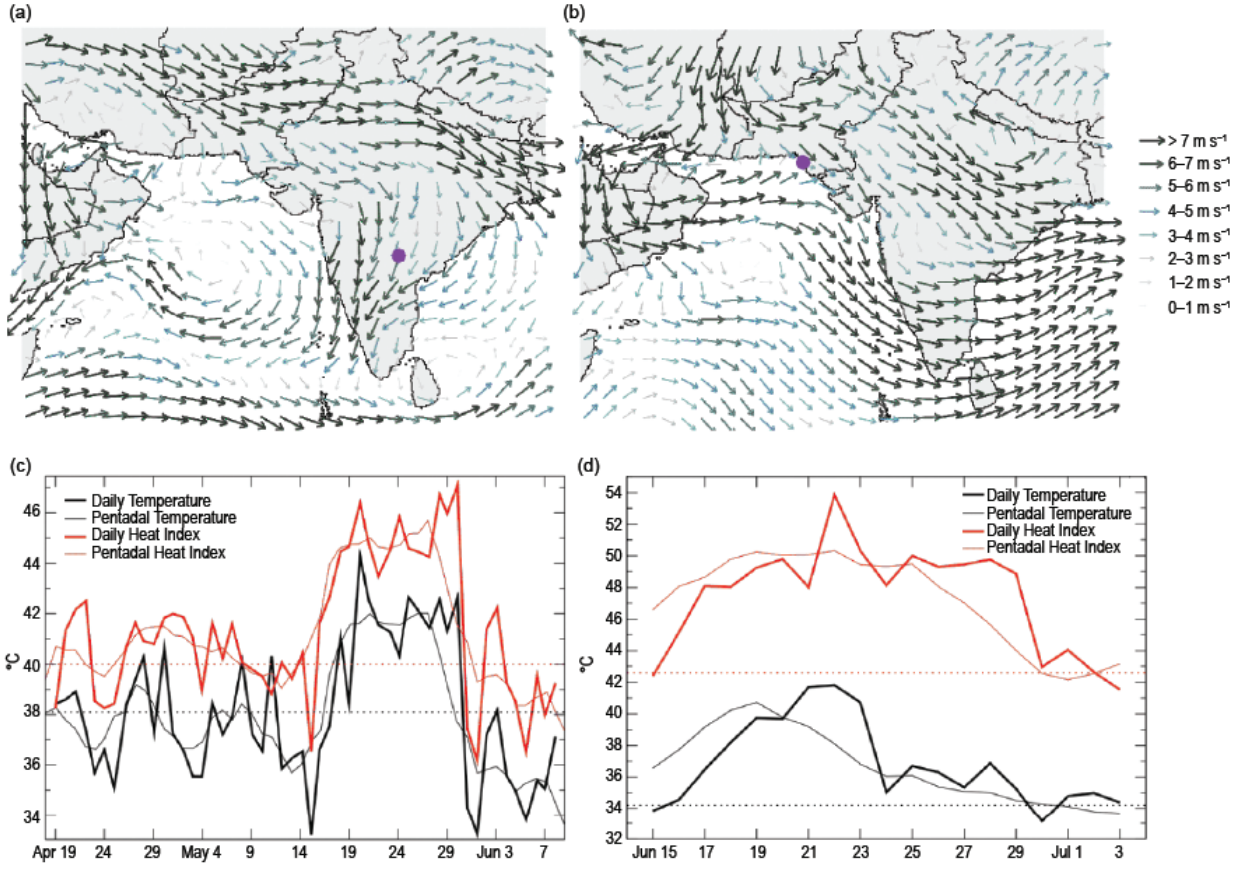

Fig. 16.1. (a),(b) Afternoon 700 hPa wind vectors and speed from the ERA-Interim reanalysis on (a) 29 May 2015 (Indian heat wave) and (b) same on 30 Jun 2015 (Pakistani heat wave). The purple dots indicate the location of the weather stations used in this study. (c),(d) Daily maximum heat index values and associated temperatures during (c) the Indian heat wave and (d) same for the Pakistani heat wave. Dotted horizontal lines are 1974–2014 climatological averages for the month of the occurrence of the peak in the heat waves.

mum heat index (indicated by the large black dot) is well within the advisory levels revealing that these U.S.-based statements were not developed for these regions. More widely applicable measures of the threat of severe heat wave to human health are not available (Wehner et al. 2016). Rare and dangerous events are along the upper-right edge of this two-dimensional distribution, which are not necessarily the highest temperatures. The 2015 heat waves are represented by asterisks. These figures reveal stark differences in both the heat waves and climatologies of the two cities. In Hyderabad, the 2015 heat wave was among the highest temperatures ever experienced but relative humidity was low, around 20%. In Karachi, the 2015 heat wave was hot but not near record levels. However, because relative humidity was high (35%–70%), the daily maximum heat indices were among the highest ever experienced. These combinations of temperature and relative humidity were rare events as is evident by the proximity of the asterisks to the edge of the distribution in Fig. 16.2b.

Analysis of possible human influence. The annual maxima of the pentadal average of the daily maximum heat indices and associated temperatures exhibit increasing trends for both stations (thin red lines in Supplemental Figs. S16.1a,b). To account for this, we use a nonstationary peaks over threshold extreme value methodology (Coles 2001) to fit a generalized Pareto distribution in order to estimate time-dependent return periods for high daily and pentadal values. To incorporate the effect of anthropogenic climate change, we used a time varying estimate of CO_2 (see www.esrl.noaa.gov/gmd/ccgg/trends/) as the covariate in the Pareto distribution using a 95th percentile threshold and a 3-week declustering. Using the event magnitudes in the first column of Table 16.1, we find a strong time dependence of the temperature and heat index return periods (Supplemental Figs. S16.1c,d) for the pentadal values. Very little time dependence in the return periods for the daily values for the Karachi station over the duration of the observational record is found, consistent with the

Table 16.1. Estimates of observed daily maximum heat index and temperature (°C), its return period (years), the corresponding quantile bias corrected return value in simulations of the actual world, and similar simulated quantities of a counterfactual world, human-induced risk ratio and return value changes. Bias corrections of the simulated actual distributions are made at the quantile corresponding to the observed return period. The magnitudes of the quantile bias corrections are the differences between values in the column labeled "Simulated Actual RV" and "Observed Value."

		Observed Value (°C)	Observed RP (years)	Simulated Actual RV(°C)	Simulated Counter-factual RP(years)	Simulated Counter-factual RV(°C)	Simulated Risk Ratio	Simulated Δ RV
Heat Index								
Hyderabad	daily	46.9	1.9	42.5	23.6	40.7	12.1	1.7
Hyderabad	pentad	45.7	2.8	42.0	92.3	40.3	32.8	1.7
Karachi	daily	53.5	4.0	49.3	31.1	46.9	7.7	2.4
Karachi	pentad	50.4	43.9	49.1	>>1000	46.6	>1000	2.5
Temperature								
Hyderabad	daily	44.0	2.7	43.4	9.6	42.5	3.6	1.0
Hyderabad	pentad	41.8	1.8	41.7	3.3	40.8	1.9	0.9
Karachi	daily	41.9	2.1	43.0	2.7	42.5	1.3	0.5
Karachi	pentad	40.7	5.9	42.8	9.4	42.3	1.6	0.5

absence of a significant trend in the extrema of daily maxima for that station (thick lines in Supplemental Fig. S16.2b). Return periods of high temperature and head index in Hyderabad exhibit strong time dependence for both the daily and pentadal values, also consistent with relative magnitude of the trends and variations of Supplemental Fig. S16.1a. The 2015 values of return periods corresponding to estimated event magnitudes are shown in the second numeric column of Table 16.1. Because the CO_2 covariate is clearly dependent on human activities, there is a statistically significant relationship between human influence and the heat index. However, because the statistical model does not consider that unforced natural variations may be coincidental with increases in atmospheric CO_2, this statistical significance does not necessarily mean that an anthropogenic response has been detected by this analysis alone.

To more rigorously estimate a possible human influence, we utilize simulations drawn from the C20C+ Detection and Attribution Subproject (Folland et al. 2014). Temperature and relative humidity were extracted from the grid points nearest to the Hyderabad and Karachi airport weather stations from two 98-member ensemble simulations of the Community Atmospheric Model (CAM5.1) at a resolution of approximately 100 km (Risser et al. 2016, unpublished manuscript, available online at https://arxiv.org/abs/1606.08908). Simulations from 1996–2015 driven by observed sea surface temperatures and sea ice distributions represent the "world that was," referred to here as "actual." A counterfactual "world that might have been" set of simulations represents the climate system had humans not altered the composition of the atmosphere (Folland et al. 2014). In this case, an estimate of the human-induced changes to the sea surface temperature and sea ice distribution obtained from the CMIP5 models is removed from the lower boundary conditions and atmospheric trace gas and aerosol concentrations set to preindustrial values (Stone 2013). Comparison of model grid points to individual weather stations is performed with caution. Hyderabad Airport is located in the countryside well outside of the metropolitan area, and thus should be representative of temperature variations occurring on spatial scales resolved by the climate model. Karachi Airport is, however, located within the metropolitan area, and Karachi itself is a coastal city, so the climate model may not be properly resolving urban and coastal microclimate phenomena that are influencing weather at the airport. However, the pair of ensemble simulations use the same changes in land use and cover, so differences are predominantly a result of changes in atmospheric composition and ocean state rather than in the urban heat island. The model was determined to be fit for purpose by the tests outlined in Angélil et al. (2016a). Angélil et al. 2016b conclude that CAM5.1's estimates of the

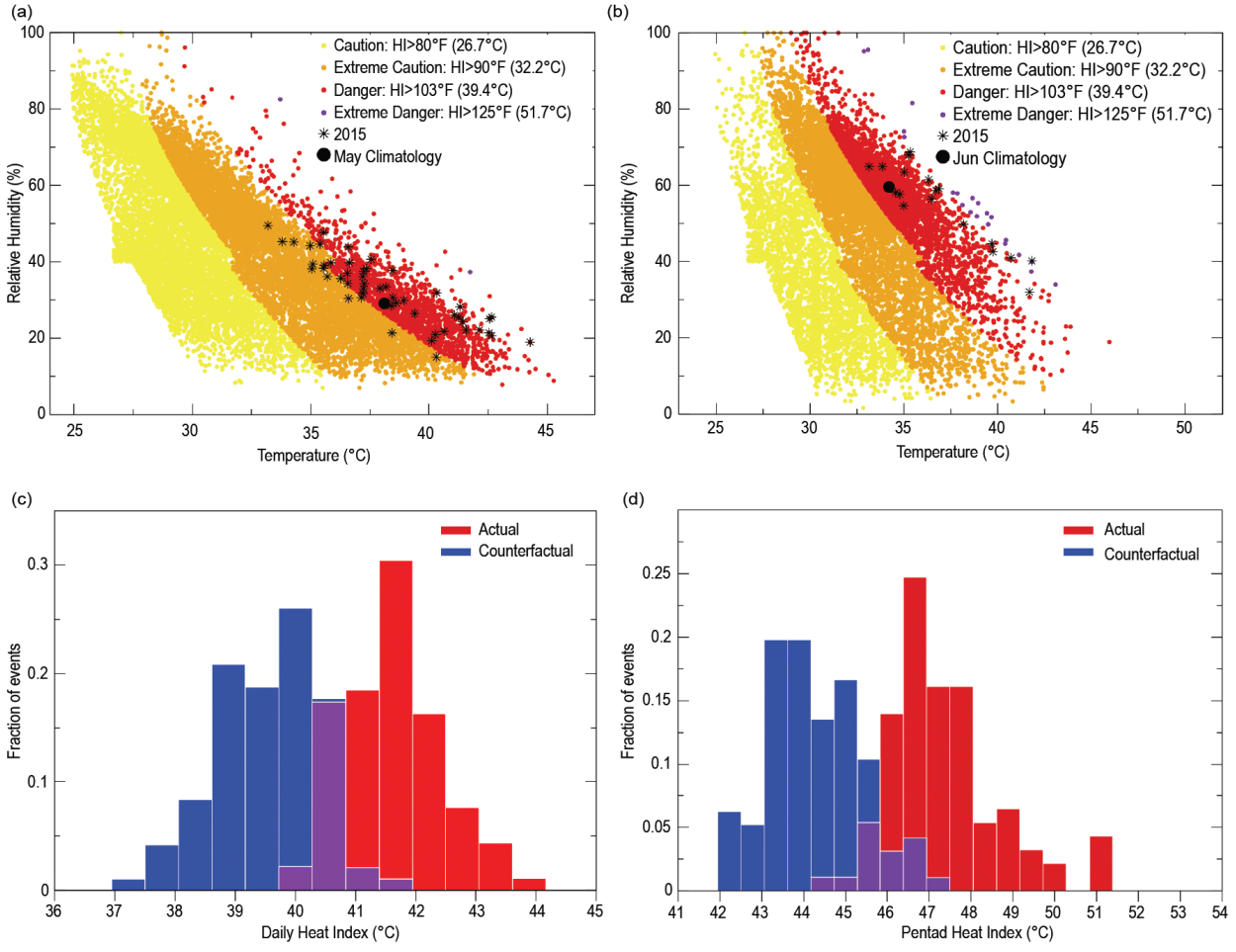

Fig. 16.2. (a),(b) Scatterplots of observed temperature and relative humidity from 1973–2015 at the time of the daily maximum heat index at (a) Hyderabad, India, and (b) Karachi, Pakistan. The 2015 heat wave days are shown by the asterisks. Other observations are colored according to NOAA heat index advisory levels. The large black dots are the May/Jun climatological averages. (c),(d) Histograms of uncorrected maximum pentadal average of daily maximum heat index for the counterfactual (blue) and actual (red) simulations, (c) May 2015, Hyderabad and (d) Jun 2015, Karachi.

1-in-1-year and 1-in-10-year anomalous thresholds for hot days over India/Pakistan are all consistent with estimates from current reanalysis products. Figures 16.2c,d show histograms approximating the simulations' distribution of the pentadal average of the daily maximum heat index for the counterfactual world (blue) and actual world (red) during the month of the two heat waves' peak intensity and reveal a pronounced shift toward higher values caused by the changes in forcing due to anthropogenic activities. Corresponding histograms for the daily maximum heat index and for both measures of extreme temperature are shown in Supplemental Fig. S16.2. For both locations, the models' response in extreme temperature is less than in heat index but the profound difference in the daily and pentadal Karachi observational extremes revealed by changes in return period (Supplemental Figs. S16.1c,d) are not readily apparent in the simulations.

Utilizing the quantile bias correction method of Jeon et al. (2015), we estimate the changes in return period for corrected daily and pentadal values of peak temperature and heat index for both heat waves. This is used to define the "risk ratio," the ratio of the probabilities of reaching the corrected model estimates of the observed event in the factual and counterfactual simulations or, more simply, the inverse of the ratio of the corresponding return periods. Shown in Table 16.1, we find a substantial human increase in the risk ratio of heat index for both the Indian and Pakistani heat waves. The heat index risk ratio is substantially larger for pentadal values than it is for daily values. This is particularly relevant to assessing human-induced changes in the heat wave-related risk

to human health and mortality, as is it is the long-term exposure to high heat that is most dangerous. Changes in simulated return values corresponding to the estimated observed return time are also shown in the last column of Table 16.1, revealing large human-induced changes in the magnitude of heat waves of a fixed rarity for both cities.

We note that the climate model simulation (not shown) does not exhibit as large a trend in the estimated return periods of temperature and heat index as some of the HadISD observational products. However, the sampling uncertainty of the observations, represented by the error bars in Supplemental Figs. S16.1c,d, is large and the model is not necessarily inconsistent with the observations in this regard. Sampling uncertainty is much lower in the model because of the size of the ensemble dampens the inherent natural variability. In the simulations, the human signal is larger for the heat index than for temperature over both the daily and pentadal extremal measures at both locations (Table 16.1). We also find that for heat index, the human influence is greater on the pentadal scales than on the daily scales but that it is about the same for temperature at both locations. The time dependence of the Karachi observations could also be described this way, although there is essentially no trend in the daily extrema (Supplemental Figs. S16.1b,d). The time dependence of the Hyderabad observations is also similar except for the large change in the daily temperature (Supplemental Figs. S16.1a,c).

Jeon et al. (2015) demonstrated that risk ratio estimates for heat waves could be relatively insensitive to uncertainty in observed event magnitude. Hence, the principal uncertainties in the estimates of risk ratio and return value changes for heat wave occurrence in Table 16.1 stem from the use of a single climate model as well as the single estimate of counterfactual ocean state rather than observational uncertainty.

Conclusion. The deadly heat waves of 2015 in India and Pakistan were distinct meteorological events without obvious connection despite the proximity in location and time. We find a substantial human-induced increase (~800% to > 100 000%) in the likelihood of the observed heat indices. Alternatively, we also find a human-induced increase (~2°C) in the heat indices of nonindustrial events of equivalent rarity to that estimated in 2015 (Table 16.1). This anthropogenic influence is found to be higher for pentadal than for daily measures of heat wave severity, with potential implications for human health and mortality because of their dependence on heat wave duration.

ACKNOWLEDGEMENT. Wehner's and Stone's contributions to this work are supported by the Regional and Global Climate Modeling Program of the Office of Biological and Environmental Research in the Department of Energy Office of Science under contract number DE-AC02-05CH11231. Castillo's contribution is supported by the National Science Foundation grant No. 000237060 under the Earth System Model (EaSM2) program.

REFERENCES

Angélil, O., and Coauthors, 2016a: Comparing regional precipitation and temperature extremes in climate model and reanalysis products. *Wea. Climate Extremes*, **13**, 35–42, doi:10.1016/j.wace.2016.07.001.

——, D. Stone, M. Wehner, C. J. Paciorek, H. Krishnan, and W. Collins, 2016b: An independent assessment of anthropogenic attribution statements for recent extreme weather events. *J. Climate*, in press, doi:10.1175/JCLI-D-16-0077.1.

Coles, S., 2001: *An Introduction to Statistical Modeling of Extreme Values*. Springer Verlag, 208 pp.

Dunn, R. J. H., K. M. Willett, P. W. Thorne, E. V. Woolley, I. Durre, A. Dai, D. E. Parker, R. S. Vose, 2012: HadISD: A quality controlled global synoptic report database for selected variables at long-term stations from 1973–2011. *Climate Past*, **8**, 1649–1679, doi:10.5194/cp-8-1649-2012.

Folland, C., D. Stone, C. Frederiksen, D. Karoly and J. Kinter, 2014: The International CLIVAR Climate of the 20th Century Plus (C20C+) Project: Report of the sixth workshop. *CLIVAR Exchanges* No. 65, **19**, 57–59.

Jeon, S., C. J. Paciorek, and M. F. Wehner, 2016: Quantile-based bias correction and uncertainty quantification of extreme event attribution statements. *Wea. Climate Extremes*, **12**, 24–32, doi:10.1016/j.wace.2016.02.001.

Masood, I., Z. Majid, S. Sohail, A. Zia, and S. Raza, 2015: The deadly heat wave of Pakistan, June 2015. *Int. J. Occup. Environ. Med*., **6**, 247–248.

Ratnam, J. V., S. K. Behera, S. B. Ratna, M. Rajeevan, and T. Yamagata, 2016: Anatomy of Indian heat waves. *Sci. Rep*. **6**, 24395, doi:10.1038/srep24395.

Salim, A., A. Ahmed, N. Ashraf, and M. Ashar, 2015: Deadly heat wave in Karachi, July 2015: Negligence or mismanagement? *Int. J. Occup. Environ. Med*., **6**, 249.

Steadman, R. G., 1979a: The assessment of sultriness. Part I: A temperature–humidity index based on human physiology and clothing science. *J. Appl. Meteor*., **18**, 861–873.

——, 1979b: The assessment of sultriness. Part II: Effects of wind, extra radiation and barometric pressure on apparent temperature. *J. Appl. Meteor*., **18**, 874–885.

Stone, D., 2013: Boundary conditions for the C20C Detection and Attribution Project: The All-Hist/est1 and Nat-Hist/CMIP5-est1 scenarios. Lawrence Berkeley National Laboratory, 18 pp. [Available online at http://portal.nersc.gov/c20c/input_data/C20C-DandA_dSSTs_All-Hist-est1_Nat-Hist-CMIP5-est1.pdf.]

Wehner, M., F. Castillo, and D. Stone, 2016: Extreme heat waves, health, and welfare in a changing climate. *Oxford Research Encyclopedia, Natural Hazard Science,* in press, doi:10.1093/acrefore/9780199389407.013.58.